2016

Groundwater transit time distribution and mean from streambed sampling in an agricultural coastal plain watershed, North Carolina, USA

Troy E. Gilmore
University of Nebraska-Lincoln, gilmore@unl.edu

David P. Genereux
North Carolina State University, genereux@ncsu.edu

D. Kip Solomon
University of Utah

John E. Solder
Utah Water Science Center

AGU PUBLICATIONS

Water Resources Research

RESEARCH ARTICLE

10.1002/2015WR017600

Key Points:
- Streambed sampling gave highly reproducible aquifer mean transit time estimates
- A gamma model best fit the observed groundwater transit time distribution
- Streambed point-scale and seepage meter sampling gave similar apparent ages

Supporting Information:
- Supporting Information S1
- Table S1

Correspondence to:
T. E. Gilmore,
gilmore@unl.edu

Citation:
Gilmore, T. E., D. P. Genereux, D. K. Solomon, and J. E. Solder (2016), Groundwater transit time distribution and mean from streambed sampling in an agricultural coastal plain watershed, North Carolina, USA, *Water Resour. Res.*, *52*, 2025–2044, doi:10.1002/2015WR017600.

Received 22 MAY 2015
Accepted 16 JAN 2016
Accepted article online 2 FEB 2016
Published online 16 MAR 2016

Groundwater transit time distribution and mean from streambed sampling in an agricultural coastal plain watershed, North Carolina, USA

Troy E. Gilmore[1,2,3], David P. Genereux[3], D. Kip Solomon[4], and John E. Solder[4,5]

[1]Department of Biological and Agricultural Engineering, North Carolina State University, Raleigh, North Carolina, USA, [2]Now at Conservation and Survey Division and Department of Biological Systems Engineering, University of Nebraska, Lincoln, Nebraska, USA, [3]Department of Marine, Earth, and Atmospheric Sciences, North Carolina State University, Raleigh, North Carolina, USA, [4]Department of Geology and Geophysics, University of Utah, Salt Lake City, Utah, USA, [5]Now at United States Geological Survey, Utah Water Science Center, Salt Lake City, Utah, USA

Abstract We measured groundwater apparent age (τ) and seepage rate (v) in a sandy streambed using point-scale sampling and seepage blankets (a novel seepage meter). We found very similar *MTT* estimates from streambed point sampling in a 58 m reach (29 years) and a 2.5 km reach (31 years). The *TTD* for groundwater discharging to the stream was best fit by a gamma distribution model and was very similar for streambed point sampling in both reaches. Between adjacent point-scale and seepage blanket samples, water from the seepage blankets was generally younger, largely because blanket samples contained a fraction of "young" stream water. Correcting blanket data for the stream water fraction brought τ estimates for most blanket samples closer to those for adjacent point samples. The *MTT* estimates from corrected blanket data were in good agreement with those from sampling streambed points adjacent to the blankets. Collectively, agreement among age-dating tracers, general accord between tracer data and piston-flow model curves, and large groundwater age gradients in the streambed, suggested that the piston flow apparent ages were reasonable estimates of the groundwater transit times for most samples. Overall, our results from two field campaigns suggest that groundwater collected in the streambed can provide reasonable estimates of apparent age of groundwater discharge, and that *MTT* can be determined from different age-dating tracers and by sampling with different groundwater collection devices. Coupled streambed point measurements of groundwater age and groundwater seepage rate represent a novel, reproducible, and effective approach to estimating aquifer *TTD* and *MTT*.

1. Introduction

Groundwater transport of legacy contaminants (e.g., excess nutrients in agricultural watersheds) into streams and rivers is a likely contributor to the lag in surface water quality improvement following nutrient management initiatives [*Meals et al.*, 2010; *Sanford and Pope*, 2013] and ecosystem restoration [*Puckett*, 2004; *Hamilton*, 2012]. This lag is linked to the distribution of groundwater transit times, that is, the travel times through the aquifer from recharge at the water table to discharge at a surface water body.

Groundwater sampling in streambeds has been used to estimate the transit time of groundwater discharging into streams [e.g., *Böhlke and Denver*, 1995; *Lindsey et al.*, 2003; *Tesoriero*, 2005; *Tesoriero et al.*, 2013] (where age at the point of discharge from the aquifer = transit time through the aquifer). *Modica et al.* [1998] showed good agreement between ages estimated by particle tracking in a groundwater flow model and tracer-based age dating of samples collected from beneath a gaining stream. Stream water sampling has also been used to determine flow-weighted concentrations of age-dating tracers in groundwater discharge to streams [*Stolp et al.*, 2010; *Solomon et al.*, 2015]. Other groundwater modeling studies have suggested that apparent groundwater age from age-dating tracers may be useful for model calibration [*Solomon and Sudicky*, 1991; *Reilly et al.*, 1994; *Portniaguine and Solomon*, 1998; *Sanford*, 2011], especially if sampling is conducted in discharge zones [*Molénat et al.*, 2013].

Traditionally, groundwater mean transit time (*MTT*) and age distributions have been evaluated by analysis of age-dating tracers in groundwater samples collected from well nests in the recharge areas of unconfined

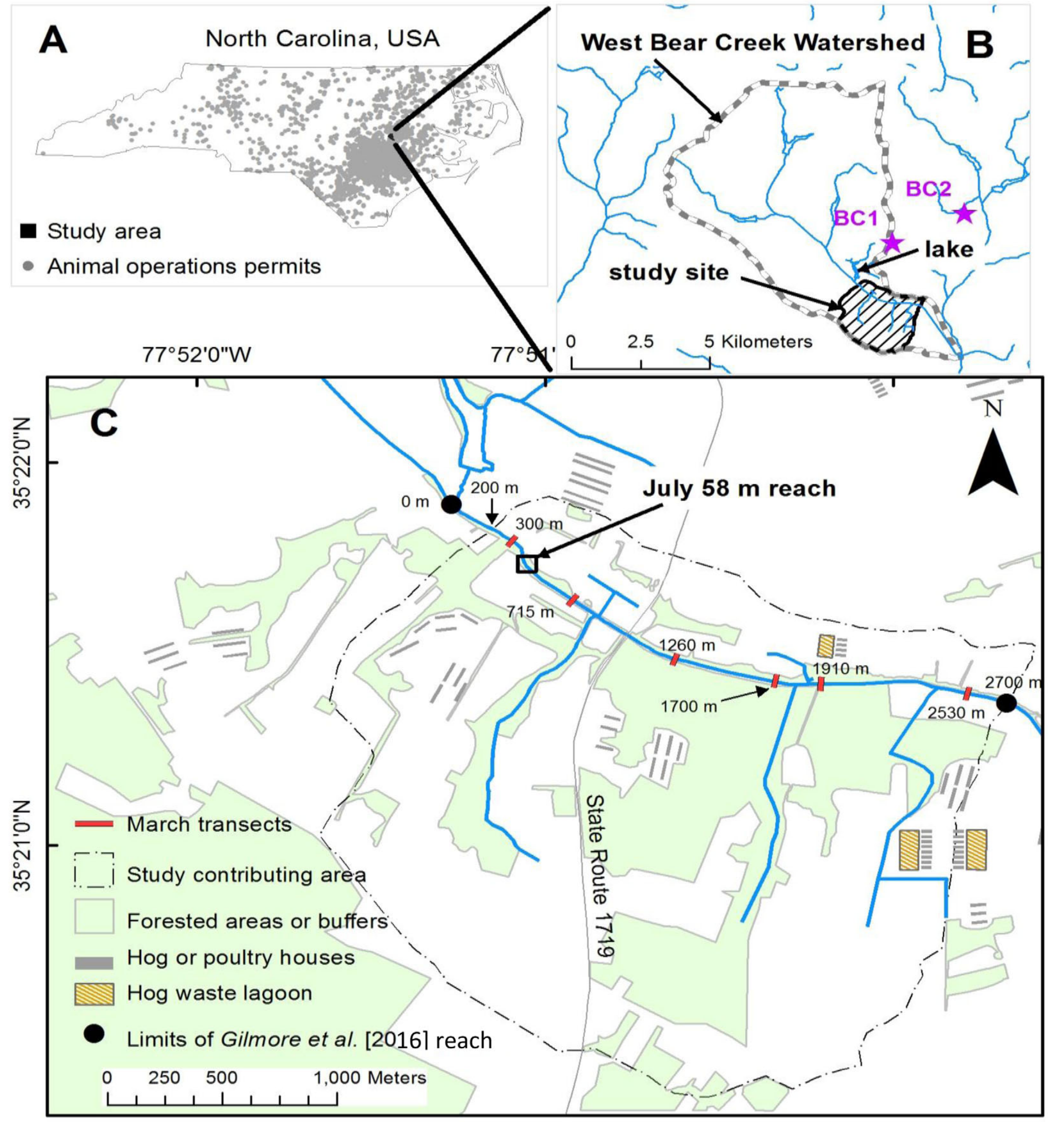

Figure 1. Study site and topographically defined contributing area for July 2012 and March 2013 field campaigns. (a) Study area location in eastern North Carolina. (b) West Bear Creek watershed is outlined by the dashed line, and the topographically defined contributing area for the 2.5 km study reach is defined by the cross-hatched area. Well nests are denoted by stars. (c) The West Bear Creek study site contributing area and sampling locations. All sampling occurred within a roughly 2.5 km reach (200–2700 m). In July 2012, all point and blanket sampling was conducted in the "July 58 m reach." In March 2013, six point transects were distributed throughout the 2.5 km reach. Seepage blanket sampling was also conducted at the 715 m transect in March. All GIS data were accessed via the NC OneMap Geospatial Portal (data.nconemap.com). Forested areas, agricultural facilities, and tributaries were defined using digital orthophotos (2010 North Carolina Statewide Digital Orthoimagery) and field observations. The contributing area for the 2.5 km reach is based on digital elevation data from the North Carolina Division of Transportation. The West Bear Creek watershed outline is from the USDA NC NRCS 12-Digit Hydrologic Units data set. The main channel of West Bear Creek and locations for animal operations permits were from data sets of the North Carolina Department of Environmental Quality (NCDEQ), formerly (before 18 September 2015) the NC Department of Environment and Natural Resources (NCDENR).

aquifers [*Solomon et al*., 2006]. Only *Browne and Guldan* [2005] and *Kennedy et al*. [2009a] have combined age estimates with groundwater flux rates at numerous points in a streambed to estimate *MTT* and transit time distribution (*TTD*) of the groundwater discharging from an aquifer to a stream. *MTT* was calculated as the flow-weighted mean apparent age of groundwater seeping through a streambed: $MTT = \Sigma v\tau / \Sigma v$, where v is groundwater seepage rate and τ is apparent groundwater age, both measured at the same location in the streambed. The *TTD* was evaluated by plotting apparent age versus the fraction of groundwater discharge. Based on streambed sampling, *Browne and Guldan* [2005] estimated an *MTT* of 24 years for

Table 1. Sampling Locations and Methods for July 2012 and March 2013 Field Campaigns

Sampling Month and Approach	Noble Gas Sampling Locations (m)	Noble Gas Sampling Technique; Container	CFC, SF_6, and Other Dissolved Gas Sample Locations (m)	CFC, SF_6, and USGS Dissolved Gas Sample Technique; Container
July 2012 points	466, 474, 481, 491, 499, 508, 516, 524	Inertial pump; copper tube	481, 516	Peristaltic pump; glass bottles
July 2012 blankets	481, 516	Peristaltic pump; copper tube	481, 516	Peristaltic pump; glass bottles
March 2013 points	300, 715, 1260, 1700, 1910, 2530	Inertial pump; copper tube	715, 1260	Peristaltic pump; glass bottles
March 2013 blankets	715	Peristaltic pump; copper tube	715	Peristaltic pump; glass bottles

groundwater in a sand and gravel aquifer 12–30 m thick [*Weeks et al*., 1965] in central Wisconsin. For the same sand-silt-clay coastal plain aquifer in which we worked (~16 m thick), *Kennedy et al*. [2009a] calculated an *MTT* of 30 years.

In this study, we went beyond previous studies in both sampling and analysis to further explore streambed sampling for groundwater age, *MTT*, and *TTD*. We collected groundwater in a coastal plain streambed using probes with 5 cm screens and analyzed the groundwater for multiple age-dating tracers (^3H, ^3He, SF_6, and CFCs) to estimate the apparent age of individual groundwater samples, and the *MTT* and *TTD* of the surficial unconfined aquifer. We investigated the effect of different streambed sampling designs on the observed aquifer *MTT* and *TTD* (point measurements closely spaced and widely spaced in stream reaches of about 60 m and 2.5 km, respectively), and sampled closer to stream banks than in previous work in an effort to more fully capture the *TTD* of the aquifer. Samples were also collected from seepage "blankets" (a novel seepage meter design [*Solder*, 2014]) deployed near a subset of point transects, an approach that could require fewer samples (and thus lower analytical costs) because each blanket integrates more streambed area compared to the screened probes. To our knowledge, groundwater age and *MTT* have not been assessed using groundwater collected by seepage meters or related streambed devices. Our related papers explore groundwater *MTT* at the reach mass balance scale based on surface water sampling [*Solomon et al*., 2015], the fate of nitrate in the surficial aquifer [*Gilmore et al*., 2016], and past and future trends in aquifer discharge of nitrate based on streambed point sampling and well sampling [*Gilmore*, 2015].

2. Study Site and Hydrologic Conditions

Our study was conducted in West Bear Creek, within a 2.5 km reach defined by *Gilmore et al*. [2016] that contained reaches previously described by *Kennedy et al*. [2007, 2008, 2009a, 2009b, 2010], *Genereux et al*. [2008], and *Solder* [2014]. The stream is deeply channelized and the sandy streambed is about 6.5 m wide. All stream locations are named by their distance in meters downstream of a tracer injection site defined as 0 m (Figure 1c); measurements were made from 200 to 2700 m. During our first sampling campaign in July 2012, stream discharge at the 200 m station (Figure 1c) was about 57 L/s, roughly an order of magnitude lower than discharge during our second field campaign in March 2013 (~500 L/s) [*Gilmore et al*., 2016].

The surficial aquifer is underlain by the Black Creek confining unit [*Winner and Coble*, 1996], the top of which is 18 m below ground surface at well nest BC1 near West Bear Creek (Figure 1b). In a separate borehole along the left bank of West Bear Creek (about 75 m upstream of the 715 m transect in Figure 1c), clayey material at a depth of about 10.6 m was interpreted as the base of the surficial aquifer [*Kennedy et al*., 2009b], possibly the Black Creek confining unit.

3. Methods

Streambed point and blanket groundwater sampling was done during 3–4 day campaigns in July 2012 and March 2013 (additional details in *Gilmore et al*. [2016] and *Solder* [2014]). Samples from 35 point locations in July 2012 and 23 point locations in March 2013 were analyzed for ^3H and ^3He. Five-point transects were closely spaced in July 2012 (eight transects within a 58 m reach of West Bear Creek), and widely spaced in

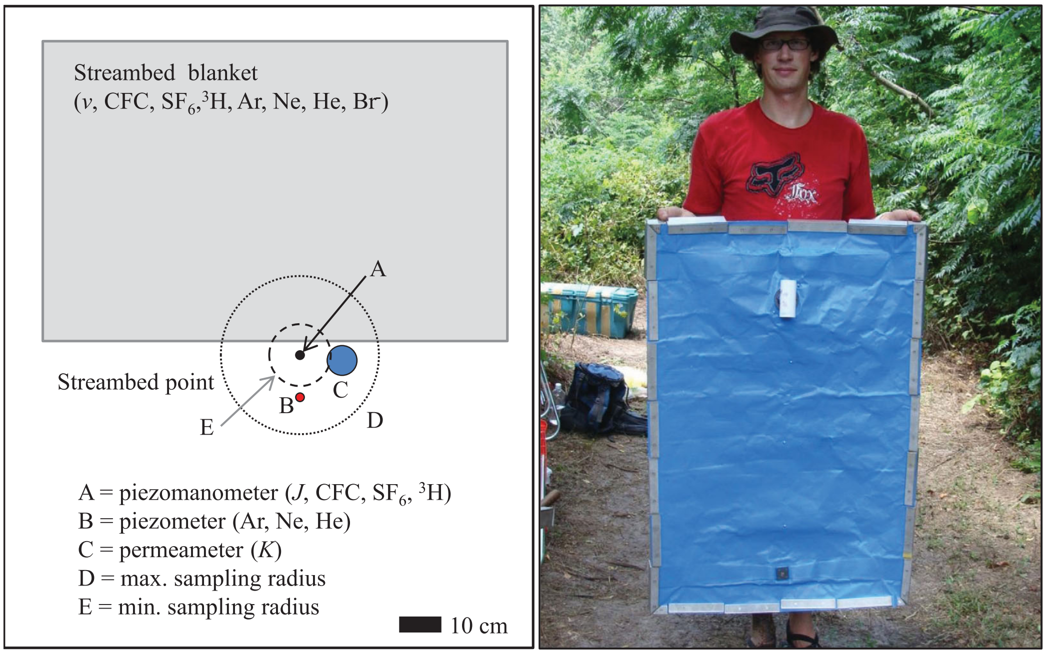

Figure 2. (left) Schematic map view of a typical streambed sampling location; each transect consisted of five such locations distributed laterally across the channel. The piezomanometer sampling radius (11–17 cm) is a rough estimate based on minimum and maximum sampling volumes for points. The point measurements were roughly centered at each blanket location (the long axis of the blanket ran across the channel). Point measurements were aligned with the downstream edge of the blanket in March 2013, while in July 2012, point measurements were made at either the upstream or downstream edge of each blanket. Photo on the right shows the top of a streambed blanket.

March 2013 (six transects spaced out over a 2.5 km reach). The positions of points in each transect were denoted as right-bank (RB), right (R), center (C), left (L), and left bank (LB). RB and LB points were located as close to the edge of the stream as feasible; fine-grained sediment derived from bank erosion made it difficult to sample within <1 m of the water line at some transects. In each field campaign, two transects were also sampled for chlorofluoromethane (CFC-11), dichlorodifluoromethane (CFC-12), trichlorotrifluoroethane (CFC-113), and sulphur hexafluoride (SF_6) in groundwater (Table 1).

At each sampling location, a piezomanometer [*Kennedy et al.*, 2007] was inserted into the streambed and purged before measuring vertical hydraulic head gradient (*J*). Groundwater samples were then collected from the piezomanometer using a syringe for nitrate or major ion samples [*Gilmore et al.*, 2016] or peristaltic pump for samples analyzed for CFC, SF_6, other dissolved gases (CH_4, CO_2, N_2, O_2, and Ar; http://water.usgs.gov/lab/), and tritium (Table 1). Piezomanometers used at CFC sampling locations were constructed of stainless steel and refrigeration grade copper, with about 30 cm of Viton® tubing in the peristaltic pump head. The screened interval for all point sampling was 31–36 cm deep in the streambed, well below the typically <10 cm deep hyphoreic zone in West Bear Creek [*Gilmore et al.*, 2016]. After sampling from the piezomanometer, a second probe (piezometer, Figure 2) was inserted into the streambed roughly 10 cm from the piezomanometer. A noble gas sample was collected from the piezometer using an inertial pump (Waterra® check-valve installed on the end of the copper tube sample container) to minimize degassing of samples during collection. Once sampling was complete, a permeameter was inserted within 10 cm to the right or left of the piezomanometer (and also about 10 cm from the location where the noble gas piezometer was inserted; Figure 2) and vertical hydraulic conductivity (*K*) was measured in the streambed [*Genereux et al.*, 2008].

Streambed blankets were installed at two transects in July 2012 (10 blankets total) and one transect in March 2013 (5 blankets) (Table 1). Streambed blankets are low-profile rectangular (71 cm $\times$ 107 cm) seepage meters constructed of flexible rubber material and lined with stainless steel foil to avoid sorption of CFCs to the rubber material [*Solder*, 2014]. A dilution flow meter was used to measure groundwater seepage rate at each blanket [*Solder*, 2014]. A complete five-blanket transect covered the streambed almost fully from waterline to waterline. Groundwater samples were collected from the blankets after measuring blanket discharge. Samples were pumped from each blanket at a flow rate that was lower than the field estimate of ambient groundwater discharge from the blanket. In some cases, blanket discharge was very low and no sample was collected (715LB in March 2013) or only a subset of samples was collected (522L in July 2012).

Water samples for noble gas analysis (Xe, Kr, Ar, Ne, and He) were collected in copper tubes sealed with steel pinch clamps [*Aeschbach-Hertig and Solomon*, 2013]. Water samples for tritium analysis were collected in 500 mL HDPE bottles. Tritium and noble gas samples were analyzed at the Dissolved and Noble Gas Laboratory at the University of Utah in Salt Lake City, UT. Groundwater samples for analysis of SF_6, CFCs, and other dissolved gases (CH_4, CO_2, N_2, O_2, and Ar) were analyzed at the USGS CFC Lab in Reston, VA.

4. Modeling

4.1. Groundwater Flux

Vertical groundwater flux (seepage rate) was determined at each point sampling location as $v=KJ$, where K (m/d) is hydraulic conductivity and J (dimensionless) is hydraulic head gradient. Volumetric water discharge from each streambed blanket was measured using a dilution flow meter [*Solder*, 2014], then divided by the streambed area covered by the blanket (0.76 m^2) to determine v. Two water fluxes were calculated for each blanket measurement: "uncorrected" and "corrected." Uncorrected flux was the total water discharge from the blanket, which could include groundwater plus any stream water that entered the blanket through hyphoreic flow paths. Corrected blanket flux was an estimate of just the groundwater flux from the blanket; to obtain the corrected flux, the stream water component of the uncorrected flux was estimated from a chemical mixing model and then subtracted from the uncorrected flux. Br^- was injected into the stream as part of a reach mass balance experiment that was concurrent with the streambed blanket and point sampling (injection details are in *Solomon et al*. [2015] and *Gilmore et al*. [2016], and the relative timing of injection and blanket sampling are shown in Figure 2 of the latter). The concentration of Br^- in the stream was at a plateau for at least 12 h prior to the time that blankets were sampled, giving the stream water component of blanket samples a known Br^- concentration. The fraction of blanket flux derived from groundwater was calculated as:

$$F_{gw}=\frac{[Br^-]_{blanket}-[Br^-]_{sw}}{[Br^-]_{gw}-[Br^-]_{sw}} \tag{1}$$

where F_{gw} is the fraction of blanket discharge that was groundwater, and the subscripts *blanket, sw,* and *gw* represent the blanket discharge, stream water, and groundwater, respectively. With F_{gw} known, corrected blanket flux was calculated as $v_{gw}=v_{blanket}F_{gw}$, where v_{gw} and $v_{blanket}$ are the groundwater flux and the total water flux from the blanket, respectively.

Corrected and uncorrected concentrations for dissolved gases (He, Ne, Ar, SF_6, and CFCs) and ^3H were also calculated for the water samples from blankets:

$$C_{gw}=\frac{C_{blanket}-\left(1-F_{gw}\right)C_{sw}}{F_{gw}} \tag{2}$$

where C is the solute concentration and the subscript *gw* indicates a corrected blanket value (i.e., a groundwater value). Uncorrected and corrected concentrations were then used to model uncorrected and corrected apparent groundwater ages.

4.2. Apparent Groundwater Age and Mean Transit Time

A slightly modified form of the closed-system equilibration (CE) model [*Aeschbach-Hertig et al*., 2008] was fit to noble gas (Ar, Ne) data to model groundwater concentrations of He, SF_6, and CFCs at the time of recharge, which were then used to determine apparent groundwater age. Apparent groundwater age is an estimate based on the concentrations of age-dating tracers in a groundwater sample, which are assumed to have been transported with that groundwater from recharge until sampling, unaffected by processes such as mixing, dispersion, matrix diffusion, and degradation [*Plummer et al*., 2006]. The model formulation we used was:

$$C_{i\text{-}mod}=\frac{C_i^{eq}(1+AH_{i-rech})}{(1+BH_{i-sam})} \tag{3}$$

where $C_{i\text{-}mod}$ is the modeled concentration of gas *i* (Ne, Ar), C_i^{eq} is the solubility equilibrium concentration of gas *i* at recharge conditions (recharge temperature, salinity, and atmospheric pressure), $H_{i\text{-}rech}$ and $H_{i\text{-}sam}$ are the Henry's Law constants for gas *i* at recharge conditions and sampling (discharge) conditions, respectively, and A and B are gas to water volume ratios in pore space at recharge and discharge, respectively [*Aeschbach-Hertig et al*., 2008]. Equation (3) differs from the usual formulation of the CE model, because variables are distinguished as representing either recharge or sampling conditions (e.g., $H_{i\text{-}rech}$ versus $H_{i\text{-}sam}$), and values of A and B were adjusted based on estimates of excess air and degassing, as discussed below.

Equation (3) was applied according to *Gilmore et al*. [2016]. Samples were categorized as having "excess air" if dissolved [Ne] (or [Ar], if [Ne] was not available) was greater than solubility equilibrium at the recharge temperature, i.e., if ΔNe was positive, where $\Delta\text{Ne}=[\text{Ne}_{meas}]/[\text{Ne}_i^{eq}]-1$, and "meas" = measured concentration in the groundwater sample. Alternately, the sample was considered "degassed" if [Ne] was lower than solubility equilibrium (negative ΔNe) (30 of 35 samples were degassed in July, and 10 of 23 samples in March 2013, with mean ΔNe of −18% and +4% for the two campaigns, respectively). For samples with excess air, we set B = 0 and calculated the value of parameter A that gave the best fit to measured [Ar] and [Ne] in the sample. The assumption of B = 0 simplified equation (3) to an unfractionated excess air (UA) model (special case of the more general CE model).

For degassed samples, we set A equal to 2.3 mL air per L water and calculated the value of parameter B that gave the best fit to measured [Ar] and [Ne] in the sample. A 2.3 mL/L was the mean A value from modeling the dissolved gas data (Xe, Kr, Ar, and Ne) from the nearby well nests (Figure 1b). The recharge temperature (12.8°C) used to calculate C_i^{eq} was based on noble gas thermometry [e.g., *Aeschbach-Hertig and Solomon*, 2013] that involved fitting the dissolved gas data from well samples to the UA model (details in *Gilmore et al*. [2016] and *Gilmore* [2015]). Only [Ar] and [Ne] were used in the model because Xe and Kr were injected into the stream as part of a reach mass balance experiment that coincided with the point and blanket sampling [*Gilmore et al*., 2016]. Solubility equilibrium concentrations were calculated using solubility equations for Ne [*Weiss*, 1971] and Ar [*Weiss*, 1970].

Building on He-^{3}H relations shown previously [*Schlosser et al*., 1988; *Solomon et al*., 1993], tritiogenic helium, [$^3\text{He}_{trit}$], was calculated as:

$$[^3\text{He}_{trit}]=\left([^4\text{He}_{meas}]R_{meas}-\alpha[^4\text{He}_{mod}]R_{atm}-[^4\text{He}_{terr}]R_{terr}\right)(1+BH_{sam}) \tag{4}$$

where subscripts *meas, mod, atm,* and *terr* represent measured, modeled, atmospheric, and terrigenic source or concentration, respectively, *R* is the [^{3}He]/[^{4}He] ratio, and α is the isotope fractionation factor (0.983) for ^{3}He and ^{4}He (R_{gas}/R_{water}). [$^4\text{He}_{terr}$] was calculated as [$^4\text{He}_{meas}$] – [$^4\text{He}_{mod}$]. Equation (4) assumes that degassing occurred in the discharge area (degassing was not detected in dissolved gas data from recharge area wells, suggesting degassing likely occurred near the stream [*Gilmore et al*., 2016; *Gilmore*, 2015]). The factor (1+*BH*) is a correction factor for degassing [*Aeschbach-Hertig et al*., 2008] at sampling conditions (subscript *sam*). R_{terr} was assumed to be 2.0×10^{-8} [*Schlosser et al*., 1988; *Solomon et al*., 1993]. Solubility of He was calculated according to *Weiss* [1971]. Given [$^3\text{He}_{trit}$] and [^{3}H], apparent age (τ) was calculated according to the standard ^{3}H-^{3}He age equation [e.g., *Poreda et al*., 1988].

A and B parameters were used to convert the measured CFC or SF_6 concentrations to an atmospheric mixing ratio (x_i, pptv) as follows [*Friedrich et al*., 2013]:

$$x_i=\frac{C_{i-sam}K_{i-rech}(1+BH_{i-sam})}{(P_a+p_{H_2O})(1+AH_{i-rech})} \tag{5}$$

where $C_{i\text{-}sam}$ is the concentration of gas *i* in groundwater, $K_{i\text{-}rech}$ is the Henry's Law constant at the recharge temperature and salinity in units of kg atm/mol, P_a is atmospheric pressure at the recharge elevation and temperature (atm), and p_{H_2O} is water vapor pressure at the recharge temperature and salinity. Mixing ratios calculated from equation (5) were matched to historical records of CFCs and SF_6 in the atmosphere (http://water.usgs.gov/lab/software/air_curve/index.html) to determine recharge year, and apparent groundwater age was calculated by subtracting the recharge year from the sampling date. SF_6 and CFC solubilities were calculated according to *Bullister et al*. [2002] and *Plummer and Busenberg* [2000], respectively.

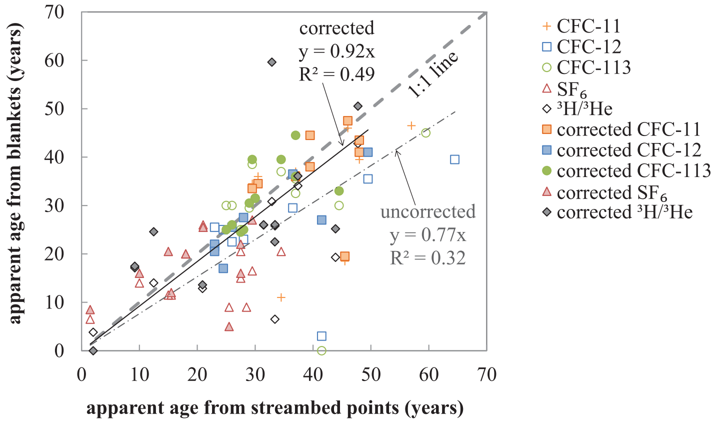

Figure 3. Relationship between apparent age of groundwater from streambed point sampling and from streambed seepage blankets. Apparent ages are from $^3H/^3He$, SF_6, CFC-11, CFC-12, and CFC-113 age-dating methods. "Corrected" indicates that apparent age from corrected blanket data is plotted against apparent age from points. Equations shown in figure are for regressions fit through the origin.

Uncertainty in apparent groundwater age from equations (3) and (5) was assessed for a subset of point samples (those from the 516 m transect, where apparent groundwater age ranged from about 2 to 41 years) using a Monte Carlo approach. For each iteration, (1) input variables were randomly varied ([Ne], [Ar], [He], [SF_6], [^3H], and recharge temperature), (2) [Ne] and [Ar] data were fit to equation (3) and either A or B was optimized, and (3) new apparent age estimates were calculated according to equations (4) and (5). Random variation in the input variables was imposed using the NORM.INV(rand(), mean, range) function in Excel®, where "range" for concentrations was set equal to their analytical uncertainty and "range" for recharge temperature was set to the standard deviation in recharge temperature estimates derived from noble gas thermometry. We also evaluated the uncertainty in apparent ages as a result of using recharge temperature and excess air values derived from well data, and sensitivity of $^3H/^3He$ apparent age to the value of R_{terr}. We also explored the potential for bias in $^3H/^3He$ apparent age if our assumption that degassing occurred at sampling was incorrect. Uncertainty in apparent age from $^3H/^3He$ was on the order of 2–6 years (where older apparent age gave the lowest uncertainties), and uncertainty in *MTT* was estimated at about 15–20%. Uncertainty in SF_6 apparent age due to recharge parameters was lower ($\leq$7%, supporting information). Factors that could increase uncertainty, but were not explored quantitatively, are mixing effects, diffusive fractionation, and for SF_6, subsurface production and local variation of input concentrations (though we do not suspect that the latter two topics are an issue near our coastal plain field site [*Busenberg and Plummer*, 2000]).

We used a Monte Carlo approach to gauge uncertainty in SF_6, ^3H, and $^3H_{trit}$ tracer concentrations and $^3H/^3He$ age estimates from the blanket mixing model calculations (equations (1) and (2)). Input variables were randomly varied using the NORM.INV(rand(), mean, range) function in Excel®, where "range" was set equal to analytical uncertainties (SF_6, ^3H) or model uncertainty ($^3He_{trit}$). Estimated uncertainty in corrected blanket SF_6, ^3H, $^3He_{trit}$, and $^3H/^3He$ age ranged from 3 to 176% and was about 30% on average. With the exception of one or two high uncertainty values associated with each of the three tracers, uncertainties averaged about 13–24%. Details of all uncertainty analyses are given in supporting information.

Apparent groundwater ages were weighted by groundwater discharge (v) from points or blankets to determine groundwater *MTT* through the surficial aquifer ($MTT=\Sigma v\tau/\Sigma v$) [*Kennedy et al*., 2009a].

5. Results

5.1. Apparent Groundwater Ages

Piston-flow groundwater ages from point and blanket sampling ranged from modern (<3 years) to about 70 years (supporting information). Relative to streambed point results, uncorrected results from streambed blankets showed a bias toward younger apparent age (blanket age = 0.57 × (point age) + 7.3 years, $R^2 = 0.37$, p-slope < 0.01). Correcting blanket data (unmixing the stream water to isolate the groundwater in blanket samples) improved agreement between blanket and point sampling, but still gave a slope of less than one (age from corrected blanket samples = 0.74 × (point age) + 6.1 years, $R^2 = 0.53$, p-slope < 0.01). Slopes were closer to one for both uncorrected blanket results (0.77) and corrected blanket results (0.92) when the regression was forced through the origin (Figure 3).

Table 2. Groundwater Fractions, F_{gw}, in Blanket Samples in July 2012 and March 2013

Sample	F_{gw}
July 2012	
481RB	0.91
481R	0.52
481C	0.89
481L	1.06[a]
481LB	0.87
516RB	0.97
516R	1.02[a]
516C	0.41
516L	0.35
516LB	0.55
March 2013	
715RB	0.16
715R	0.74
715C	0.38
715L	0.52
715LB	no sample

[a] F_{GW} was considered equal to 1.00.

We determined apparent ages from dissolved gases in stream water collected near the streambed blankets in March 2013 ($^3H/^3He$ age = 2.2 years, SF_6 age = 4.5 years) and July 2012 ($^3H/^3He$ age = 13.6 years, SF_6 age = 8.0 years). These apparent ages are not true ages of stream water, but suggest that uncorrected blanket ages are younger than corrected blanket ages because stream water is relatively "young" with respect to its age-dating tracer signatures, due to partial in-stream reequilibration with the atmosphere [*Solomon et al*., 2015]. Groundwater fractions in blanket samples were determined from equations (1) and (2) and ranged from 0.16 to 1.0, where a fraction of 1.0 indicates that no stream water was detected in the blanket sample (Table 2).

There were more large point-blanket differences (>15 years) for uncorrected blanket ages (7) than for corrected blanket ages (4), and a larger mean difference (6.1 years for uncorrected compared to 1.3 years for corrected). Overall, the difference in the mean apparent age was statistically significant ($p < 0.01$; standard two-tailed t test) for points versus uncorrected blankets but not points versus corrected blankets ($p = 0.52$). It seems clear that correcting the blanket data improved agreement between points and blankets, but after correcting blanket data there were fewer blanket results that could be compared with points (49 instead of 56), because (1) some corrections resulted in negative groundwater concentrations for SF_6 and/or CFCs (sites 481R, 715RB) and (2) some corrected concentrations showed contamination of CFCs (sites 715RB, 715C).

Overall, we focus mainly on $^3H/^3He$ apparent ages because these data were available for many more sampling locations (23 points in March, 35 in July) compared to SF_6 or CFCs ($n \leq 10$ points). The strongest agreement in groundwater apparent age between age-dating tracers was for SF_6 and $^3H/^3He$ from the March 2013 campaign, where degassing was less prevalent (43% of samples) compared to July 2012 (85% of samples). Production of biogenic gases was a likely driver of degassing [*Gilmore et al*., 2016], and lower hydrostatic pressure as groundwater approached the streambed (e.g., sampling roughly 0.5–1.0 m below stream surface) likely contributed to the formation of bubbles and subsequent degassing. Degassing can be accounted for by using noble gas modeling, but sampling in colder conditions when gas solubility is higher may minimize degassing, particularly in areas where biogenic gas production is prevalent (e.g., agricultural areas). We believe $^3H/^3He$ gave the most robust age estimates for degassed samples, as possible fractionation in some July 2012 samples may have caused SF_6 concentrations to be overcorrected. Relative to $^3H/^3He$, apparent ages from CFCs generally seemed to be affected by either contamination or degradation (supplemental information).

5.2. Groundwater Flux Used in *MTT* and *TTD* Calculations

Groundwater flux estimates needed for calculation of *MTT* and *TTD* ranged from <0.002 cm/d to 4.4 m/d, similar to the range observed in 422 measurements by *Kennedy et al*. [2009b]. Mean groundwater flux based on point measurements was 0.35 m/d ($n = 39$) in July 2012 and 0.40 m/d ($n = 30$) in March 2013. In July 2012, uncorrected and corrected water fluxes from blankets seemed anomalously low ($v = 0.1$ and 0.07, respectively) compared to adjacent point measurements ($v = 0.63$ m/d, $n = 10$), but the blanket estimates followed the same pattern across the stream (higher v in the center) as point measurements. In March 2013, blanket fluxes (0.49 m/d uncorrected, 0.23 m/d corrected) were similar to adjacent point measurements (0.31 m/d). *Solder* [2014] and *Gilmore et al*. [2016] provide additional details.

5.3. Groundwater Mean Transit Times

Groundwater sampling by the point approach was conducted during different seasons, under different streamflow conditions, at different streambed locations and using different sampling designs and densities (Table 3), but the *MTT* determined by $^3H/^3He$ showed close agreement between July 2012 (29 years) and March 2013 (31 years). These *MTT* values were also similar to another *MTT* estimate from previous work in West Bear Creek: 30 years [*Kennedy et al*., 2009a], based on a different age-dating tracer (CFCs, mainly CFC-12) and

Table 3. MTT Results From Three Streambed Point Sampling Campaigns in West Bear Creek, and From Nearby Well Nests

	July 2012	March 2013	April 2007[a]	June 2013[b]
MTT (years)	29	31	30	27
Age-dating method	$^3H/^3He$	$^3H/^3He$	CFC	$^3H/^3He$, SF_6
Number of sampling points[c]	35	23	21	6
Points per transect	5	5	3	n.a.
Sampling density (points/m^2)	0.09	0.002	0.04	n.a.
Distance between transects (m)	8.3	800–900	12.5	n.a.
Location in WBC[d] (m)	466–524	300–2530	613–688	Near WBC
WBC stream discharge[e] (L/s)	57	504	Low flow[f]	n.a.
USGS BC stream discharge[g] (m^3/s)	0.5	1.8	0.8	3.6

[a] *Kennedy et al.* [2009a].
[b] *Gilmore* [2015]; two well nests (Figure 1) with three wells in each nest.
[c] In July 2012 and March 2013, some samples were lost during analysis or gave anomalous noble gas concentrations. For wells, a total of 12 ages (3 wells × 2 well nests × 2 tracers) were estimated. *MTT* was modeled for each well nest (based on ages from SF_6 and $^3H/^3He$ at each nest) and the mean value is shown here.
[d] meters downstream of the "0 m" site in West Bear Creek (WBC) (Figure 1).
[e] Discharge at 200 m station in West Bear Creek.
[f] Streamflow was lower than long-term median flow at nearest USGS stream gauge [*Kennedy et al.*, 2009a].
[g] Bear Creek (BC) stream discharge at USGS stream gauge at Mays Store, NC, during the middle of the sampling period (http://waterdata.usgs.gov/nwis/uv?site_no=0208925200).

streambed sampling design (Table 3). The three estimates of *MTT* from streambed sampling were slightly greater than the *MTT* modeled from groundwater age versus depth relationships observed in nearby well nests (Figure 1), which was about 27 years based on $^3H/^3He$ and SF_6 [*Gilmore,* 2015]. *MTT* determined from a reach-mass balance approach (estimating the mean SF_6 concentration in groundwater discharge from measured SF_6 concentrations in stream water) was also about 27 years [*Solomon et al.*, 2015].

MTT values from corrected blanket data were generally in good agreement with those based on point measurements adjacent to the blanket locations (1.2–5.2 years different for cases where $n > 2$, rows B versus C and F versus G, Table 4). These differences were similar and in some cases less than differences in *MTT* between different age-dating tracers in July 2012 (e.g., 1.3–19.5 years in July 2012, Row D in Table 4).

5.4. Transit Time Distribution From Streambed Point Samples

When $^3H/^3He$ groundwater ages from streambed point sampling are weighted by groundwater flux [e.g., *Browne and Guldan*, 2005; *Kennedy et al*., 2009a], the shape of the cumulative *TTD* [e.g., *Visser et al*., 2013] is very similar for the July 2012 and March 2013 field campaigns (Figure 4). Data show that about 76% of the groundwater discharging into West Bear Creek had apparent age of 20–40 years, with 11–12% of discharge having <20 year apparent age, and about 13% of discharge in the 40–60 year range. *Kennedy et al*. [2009a]

Table 4. Mean Transit Times Determined by $^3H/^3He$, SF_6, and CFC Age-Dating Methods

Row	Sample Type	$^3H/^3He$	SF_6	CFC-11[a]	CFC-12[b]	CFC-113[a]
		July 2012 Mean Transit Time in Years (# Samples[c])				
A	Points	29.2 (35)	26.4 (10)	45.2 (10)	36.0 (6)	38.5 (10)
B	Points at corr. blankets	35.0 (9)	24.0 (8)	41.3 (8)	27.0 (4)	32.0 (8)
C	Corrected blankets	30.2 (9)	18.8 (8)	40.1 (8)	23.5 (4)	34.7 (8)
D	Points with all tracers[d]	38.1 (5)	25.5 (5)	43.7 (5)	24.2 (5)	33.8 (5)
		March 2013 Mean Transit Time in Years (# Samples[c])				
E	Points	31.0 (23)	31.7 (9)	46.8 (10)	50.2 (9)	45.7 (10)
F	Points at corr. blankets	15.6 (2)	12.9 (2)	45.5 (1)	31.9 (4)	29.9 (3)
G	Corrected blankets	24.0 (2)	13.8 (2)	19.5 (1[e])	32.8 (4)	28.7 (3[e])
H	Points with all tracers[d]	30.8 (6)	32.3 (6)	47.6 (6)	52.2 (6)	47.3 (6)

[a] *MTT* from CFC-11 and CFC-113 are believed to be affected by sorption or microbial degradation in the surficial aquifer; see supporting information.
[b] CFC-12 was contaminated in 4 of 10 samples in July 2012.
[c] Number of samples varies between "points at blankets," "corrected blankets," and "blankets" due to samples lost during transport or analysis, noble gas concentrations that were 2X–3X different than expected based on the mean concentration for the given campaign, contamination of CFCs, or due to impossible negative groundwater concentrations calculated from blanket corrections.
[d] Mean transit times from point sampling locations where apparent age was able to be determined from all five available age-dating tracers.
[e] CFC-11 and CFC-113 results suggested contamination in one or more blanket samples.

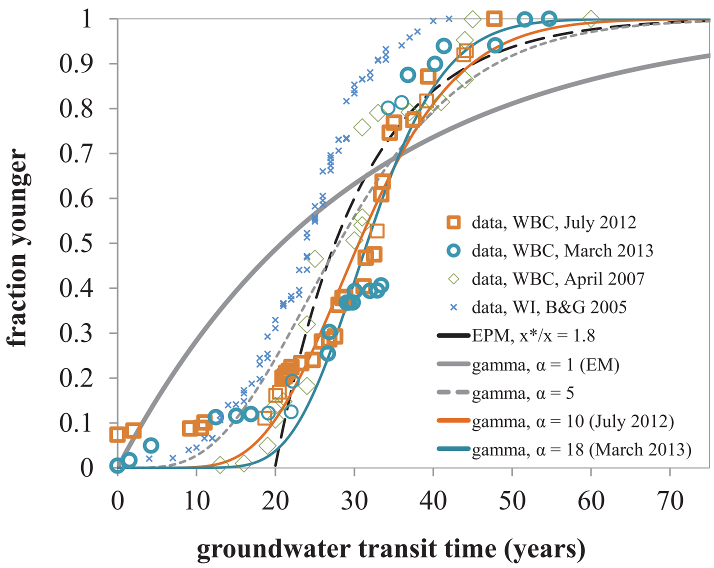

Figure 4. The cumulative transit time distribution of groundwater discharging through the West Bear Creek (WBC) streambed in April 2007 [*Kennedy et al.*, 2009a], July 2012, and March 2013. Data from streambed sampling in Wisconsin ("B&G 2005," for *Browne and Guldan* [2005]) are also shown. Apparent groundwater age values are based on streambed point sampling, for CFCs [*Browne and Guldan*, 2005; *Kennedy et al.*, 2009a], and for $^3H/^3He$ (July 2012 and March 2013 data in the present study, with SF_6 used where $^3H/^3He$ was unavailable: one sample in July and three in March). Curves show *TTD* predicted by an exponential-piston flow model (EPM), or gamma distribution ("gamma," with α ranging from 1 to 18, where $\alpha = 1$ is equivalent to an exponential model (EM)).

also observed a high percentage (66%) of groundwater with apparent CFC age of 20–40 years, based on 21 point samples collected in the streambed of West Bear Creek in April 2007 (when stream discharge was intermediate compared to July 2012 and March 2013) (Figure 4).

The high degree of reproducibility among the three streambed point sampling campaigns suggests that the *TTD* and *MTT* of groundwater discharging through the streambed are highly steady and stationary parameters at West Bear Creek, and that given enough samples (>20 for these three cases), the streambed sampling approach is robust (i.e., outcomes are not sensitive to the spacing or locations of point transects, hydrologic conditions during sampling, and perhaps even the choice of age-dating tracer, though local contamination and falling atmospheric mixing ratios present challenges for CFC dating).

When we plotted age results from groundwater sampling beneath a meandering stream channel in Wisconsin [*Browne and Guldan*, 2005] as a cumulative *TTD*, the data showed a similar shape to that observed at West Bear Creek (although shifted toward younger ages due to a lower *MTT*; Figure 4). The similarity in *TTD* shape at the Wisconsin and North Carolina sites, the only two unconfined aquifers we know of with the data needed to plot a *TTD* directly as in Figure 4, raises the question of whether the form of these observed *TTD*s is generally and broadly applicable to unconfined aquifers, and if so, why (what aquifer properties give rise to a *TTD* of this form).

The measured *TTD*s have far too little young groundwater to fit the exponential model (EM, Figure 4) distribution expected for a simple aquifer of uniform thickness and recharge [e.g., *Vogel*, 1967]. Instead, we found that the observed *TTD* more closely resembled distributions that could arise from spatial variability in recharge, such as a distribution derived from the exponential-piston flow model (EPM) [e.g., *Solomon et al.*, 2006, equation (6)], or, with a somewhat better fit, a gamma distribution [e.g., *Amin and Campana*, 1996; *Kirchner et al.*, 2010] (Figure 4).

The EPM equation

$$\tau = \frac{L\theta}{R_{EPM}} \ln\left(\frac{L}{L-z}\right) + \frac{L\theta}{R_{EPM}}\left(\frac{x*}{x}\right) \quad (6)$$

describes a flow system where groundwater is recharged in an unconfined portion of the aquifer (length $= x$) and then flows into a confined portion of the aquifer (length $= x^*$). The aquifer is assumed to have uniform thickness (L) and porosity (θ), and recharge at a rate that is steady as well as uniform in the unconfined portion (R_{EPM}). The age of groundwater (τ) increases with depth (z) in the aquifer, and the minimum age in aquifer discharge to a stream is defined by the second term in equation (6) (i.e., the age of groundwater at $z = 0$ at the aquifer discharge face equals the travel time through the confined portion of the aquifer). Equation (6) describes the age versus depth relationship in an aquifer, but the ratio of z to L is equivalent to the "fraction younger" value plotted for any given τ in Figure 4 because groundwater discharge from the aquifer is uniform over the aquifer thickness *L*.

The two-parameter gamma travel time distribution is defined by a shape factor (α) and a scaling factor (β), where $MTT=\alpha\beta$ [*Kirchner et al*., 2010, equation (6)]:

$$h(\tau)=\frac{\tau^{\alpha-1}}{\beta^{\alpha}\Gamma(\alpha)}e^{-\tau/\beta} \tag{7}$$

$\Gamma(\alpha)$ is the gamma function [e.g., *Andrews and Phillips*, 2003]. Gamma distributions with small α (e.g., $\alpha<1$) have a large fraction of young water and have been used to describe residence time distributions in catchments [e.g., *Kirchner et al*., 2000, 2010], while the gamma distribution with $\alpha=1$ is equivalent to the EM distribution (Figure 4) commonly applied to unconfined groundwater systems. In contrast to the small catchment work, the *TTDs* observed in this study are well fit by gamma distributions with large α (e.g., $\alpha\geq 5$, Figure 4), though with some underprediction at small transit times.

Best fit curves for July 2012 and March 2013 (Figure 4) were calculated in Excel® using the function GAMMA.DIST (τ, α, β, TRUE). Model parameter values for the EPM (e.g., R_{EPM}, x^*/x) and gamma distributions (α and β) were determined by using Solver® in Excel® to minimize the misfit in "fraction younger" (i.e., minimize $SSE=\Sigma(\text{observed-modeled})^2$).

Using best estimates for aquifer thickness and porosity (L = 16 m, θ = 0.35; *Gilmore* [2015]) and constraining *MTT* to a range of 29–31 years (Table 3), the EPM gave a reasonable fit to the rising limb and tail of the distribution at long transit time, if the minimum age was set equal to the average apparent age of the left bank and right bank point samples (20 years for July and March field campaigns combined; Figure 4), but the EPM fit had shortcomings. The resulting x^*/x and R_{EPM} suggested that the length scale of the confined portion of the aquifer is about 1.8 times that of the unconfined portion, and that the unconfined portion receives recharge at a rate of 50 cm/yr (both seem unrealistically large). The *SSE* was large (58), mainly due to poor fit for groundwater ages < 20 years (for ages ≥ 20 years, SSE = 0.52). With only *L* and θ constrained (all other variables in equation (6) unconstrained), the overall *SSE* was better (0.96 rather than 58), but the EPM was visually a poor fit to the observed data and suggested MTT = 40 years, well above the *MTT* estimates calculated as flow-weighted mean ages (Table 3).

Narrow constraints on the gamma distribution fitting parameters (α and β) were not necessary to achieve a good fit to the data. Compared to the EPM, the gamma distribution better fit the observed transit time distributions and had low *SSE* (0.2 for both July 2012 and March 2013 data sets). *MTT* calculated from the best fit values of α and β was 32 years for both campaigns, very close to the *MTT* values of 29–31 years calculated as flow-weighted mean ages from the point measurements (Table 3). The *MTT* of 24 years suggested by fitting the gamma model to the field data of *Browne and Guldan* [2005] (α = 10, SSE = 0.1) was the same as their reported flow-weighted mean age.

Viewed with the *TTD*s from *Browne and Guldan* [2005] and *Kennedy et al*. [2009a], the results of this study suggest that a gamma distribution with large α may be a better fit than the commonly assumed exponential distribution for the *TTD* in unconfined aquifers. For West Bear Creek, we hypothesize that the groundwater *TTD* may be influenced by spatial variability in recharge. To our knowledge, a relationship between the gamma distribution and spatial variation in recharge has not been established, but results from a preliminary 2-D groundwater model with no dispersion suggest that the *TTD* could fit the shape of a gamma distribution with $\alpha>1$ if the aquifer receives low or zero recharge near the stream and higher recharge further from the stream (details in the supporting information). Other work has drawn a connection between the value of α and watershed hydrological characteristics. For example, in a study of catchment transit times in Scotland, *Hrachowitz et al*. [2010] related the α parameter to drainage density, the presence of hydrologically responsive soils, and catchment water storage. Similar connections may exist for base flow to streams [e.g., *Kollet and Maxwell*, 2008].

Age distributions at well nests near West Bear Creek (Figure 1) suggest that recharge could vary across the contributing area [*Gilmore*, 2015]. It is possible that recharge near the stream is limited by shallow low-permeability layers like that observed in the borehole next to West Bear Creek [*Kennedy et al*., 2009a] and/or the roughly 150–200 m wide floodplain composed of poorly drained soils on each side of West Bear Creek. Conceptually, this would be similar to the distribution of age observed near a stream in Minnesota [*Böhlke* *et al*., 2002], where the groundwater system was semiconfined near the stream, and mostly older water was discharging toward the stream (although limited streambed sampling occurred in that study). Variability in recharge could also be magnified by tributaries or agricultural ditches, which may drain shallow groundwater or capture runoff (in the gently sloping floodplain) that might otherwise recharge the groundwater system. Some young groundwater may discharge from steep stream bank surfaces near the waterline (not captured by our sampling methods), while minor zones of recharge near the stream or bank storage return flows could be responsible for the small amount of 0–20 year old groundwater discharge that was observed (Figure 4).

5.5. Appropriateness of Apparent Age Estimates

When interpreting age-dating tracer data from individual groundwater samples, the key issue is whether individual groundwater samples are composed of groundwater from a narrow enough range of age such that there is insignificant bias between the apparent age and the true mean age of the sample. The available tracer data can never "prove" the exact composition of each sample, but it can be tested for consistency with the simplest model (piston flow model, PFM) by comparing apparent ages among different tracers and by using tracer plots. Additionally, the likelihood that a wide range of ages was intercepted during sampling can be assessed by considering the magnitude of groundwater age gradients (e.g., in an aquifer or across a streambed), sampling screen length, and sampling volume (Appendix A).

Results from this study indicate that discrete groundwater age information has not been completely lost by dispersion in the aquifer is the presence of large age gradients in the streambed, similar to results of *Kennedy et al*. [2009a]. The mean age gradient (calculated as the difference between groundwater ages from two streambed points divided by the horizontal distance between those two points) was about 10.6 yr/m, with a maximum of about 26 yr/m in each campaign (based primarily on ages from $^3H/^3He$, with results from SF_6 used for four points where $^3H/^3He$ was not available). Some dispersive mixing must occur during groundwater flow toward the stream but it is obviously not strong enough to homogenize age-dating tracer concentrations in groundwater beneath the stream. Also, a small amount of mixing of groundwaters of different age likely occurred in the sample bottles during and because of sampling, a fundamentally different phenomenon than the natural mixing by dispersion in the aquifer and a minor influence on individual apparent ages (Appendix A).

Another approach to assess the appropriateness of the piston-flow model (PFM) for individual point samples is to compare apparent age estimates from two or more tracers, especially when tracers exhibit different sensitivity to the piston-flow assumption (disagreement between the tracers may indicate a significant deviation from the PFM). For the March 2013 data, SF_6 and $^3H/^3He$ apparent ages were in strong agreement (supporting information). Data from July 2012 showed less agreement, but the differences between SF_6 and $^3H/^3He$ apparent ages may be explained by greater degassing in July 2012 compared to March 2013, rather than mixing of groundwaters with a wide range of transit times (supporting information).

Testing for extensive groundwater mixing has also commonly been accomplished with tracer plots (Appendix A), although some complex but more quantitative approaches have recently been explored [e.g., *Massoudieh et al*., 2012, 2014; *Green et al*., 2014]. Coupled [SF_6] and [$^3He_{trit}$] from individual points are plotted near a PFM curve (Figure A2, Appendix A) Plots comparing initial tritium ($[^3H]+[^3He_{trit}]=[^3H_{initial}]$) to ^3H concentration in precipitation showed that [$^3H_{initial}$] from only about 6 point samples (out of 58 total) differed significantly from the PFM curves (they fall about an order of magnitude below these curves, Figure A1, Appendix A) Corrected blanket data showed greater deviation from the PFM than point data, possibly as a result of greater mixing associated with blanket sampling and/or uncertainty in blanket correction calculations (supporting information). Given the large groundwater age gradients in the streambed, a general accord between age-dating tracer data and the PFM, and agreement between tracers, it seems appropriate to use the piston-flow assumption to estimate groundwater transit times, especially for the point data.

5.6. Spatial Variability in Apparent Groundwater Age

On average, $^3H/^3He$ apparent groundwater ages from point sampling showed a symmetric lateral pattern of higher age in the center of the streambed and younger apparent age toward the stream banks (Figure 5), although this pattern was not present in every point transect (Figures 5 and 7). The overall result of greater

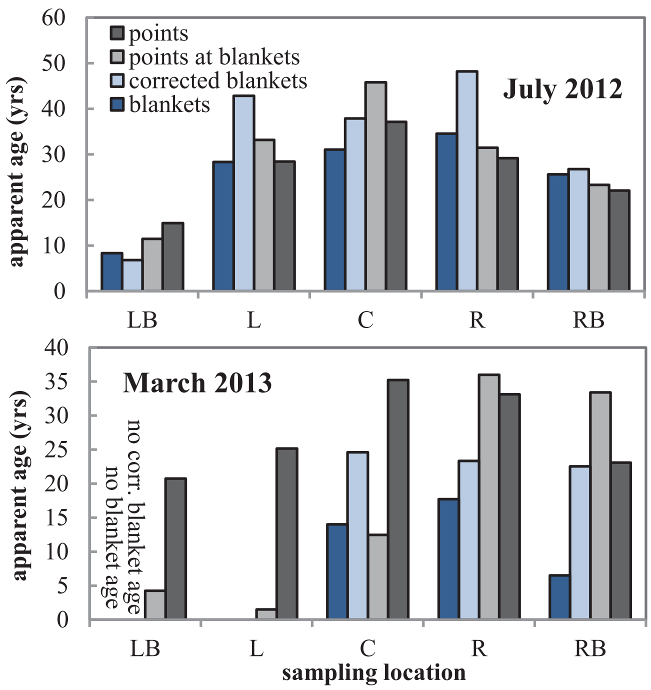

Figure 5. Lateral patterns in apparent groundwater age for streambed point and blanket transects, from left bank to right bank. Age estimates are from $^3H/^3He$. No samples were collected from the left bank (LB) blanket in March 2013. Both corrected and uncorrected blanket data from the left (L) sampling location gave negative apparent age (−3.6 and −8.4 years, respectively) from $^3H/^3He$ in March 2013, and those samples were interpreted as modern groundwater (apparent age = 0 years).

apparent ages toward the center of the stream from point samples was consistent with the conceptual model of *Modica et al.* [1998] and with the findings of *Kennedy et al.* [2009a].

The age gradients across the streambed, mentioned in the previous section, may have implications for interpreting groundwater age from streambed blanket sampling, given that each blanket integrates along a length of about 1 m in the lateral direction across the stream. For [SF_6] and/or $^3H/^3He$, the apparent age of a mixture of groundwater that spans about 10 years will result in a reasonably close estimate of the true mean age of the mixture, at least for groundwater recharged in the last 30–40 years. The likely agreement between the true age and apparent age of a groundwater mixture is because atmospheric [SF_6] has increased in a roughly linear trend for most of the last 30 years, while [^3H] in precipitation has dropped smoothly over the last 40 years (e.g., for $^3H/^3He$, the difference between apparent and "true" age was <1 year along a 10 year mixing window, Appendix A). If age gradients in the streambed are large (e.g., 20–30 yr/m), then the blanket would integrate a wider groundwater age distribution, with greater potential for bias in apparent age [e.g., *Bethke and Johnson*, 2008; *McCallum et al.*, 2014] and a greater likelihood of deviating from the tracer curves in tracer-tracer plots (e.g., [$^3He_{trit}$] versus x_{SF6} plot, Appendix A).

Two of the four blanket samples that stand out in the [$^3He_{trit}$] versus x_{SF6} plot (516L and 481L, Appendix A) were located near large groundwater age gradients in the streambed (26 and 22 yr/m, respectively). In some cases but clearly not all (e.g., 481RB, 516R; supporting information), mixing of groundwater of different ages may, like groundwater—stream water hyporheic mixing, present a complication to interpretation of groundwater age based on age-dating tracers in water samples from seepage blankets.

In July 2012, younger groundwater was observed in the lower half of the 58 m reach (Figure 6). It is possible that the detection of younger groundwater was linked to shallower conditions (average stream depths were 18 and 25 cm depth in the lower and the upper halves of the reach, respectively). The shallower conditions result in less vertical (unsampled) surface area along the edges of the stream, which may contribute to greater detection of young groundwater discharge through the more horizontal (sampled) portions of the streambed. A regression of apparent groundwater age versus stream depth from July 2012 data suggested a statistically significant relationship at the 95% confidence level ($p = 0.04$). Older groundwater was more prevalent at deeper locations, indicating that in some stream reaches, the location of the thalweg (as opposed to the "center" defined by the midpoint between the waterline on each side of the stream) could influence where the oldest water enters the stream. March 2013 point data suggested older groundwater in the lower half of the 2.5 km reach (Figure 7) at the 1700 and 1910 m transects. If some of this groundwater were recharged before 1950, the ages for those samples may be underestimated, possibly making the tail of the *TTD* in Figure 4 too short.

Overall, results from streambed point sampling in July 2012 and March 2013 show lateral patterns in groundwater apparent age that are consistent with previous work [*Kennedy et al.*, 2009a] and conceptual models [e.g., *Modica et al.*, 1998], even though the sampling scales (58 m versus 2.5 km), distances between

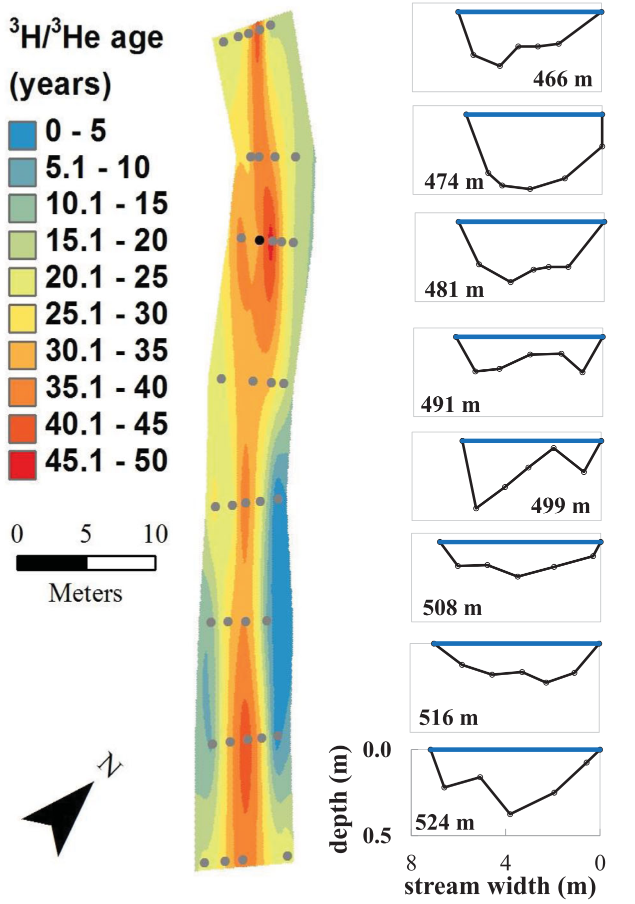

Figure 6. Map of apparent age of the groundwater discharging through the streambed of West Bear Creek, with stream depth profiles for each transect, in July 2012. Ages are from the ^{3}H/^{3}He method (grey dots on map) with the exception of one age estimated from SF_6 (black dot). The direction of streamflow is from top to bottom on the map, thus the right bank (RB) is on the left side of the map. All depth profiles were plotted at the same scale, shown with axis labels on the bottom-most plot. Depth profiles are shown in the same order as transects on the map (from upstream at the top to downstream at the bottom). Blankets were deployed along the transects at 481 and 516 m. The streambed map was created in ESRI™ ArcMap 10.0 using the multiquadric radial basis function with anisotropy ratio of 8 and smoothing parameter set = 0.

transects (8.3 m versus 800–900 m), and streamflow conditions (57 L/s versus 500 L/s) differ by at least an order of magnitude between the two sampling campaigns. Streambed point and blanket sampling seemed to capture a similar overall picture of groundwater age across the streambed, although mixing (among groundwaters and between groundwater and stream water) complicates the interpretation of age-dating tracer concentrations for some blankets (e.g., Figure 5 and Appendix A).

6. Summary and Conclusions

We used a streambed point approach and seepage meters (flexible streambed seepage "blankets") to sample groundwater discharge from the surficial aquifer to West Bear Creek in the coastal plain of North Carolina. Apparent groundwater age determined from age-dating tracers was weighted by groundwater discharge rate through the streambed to determine both the flow-weighted mean apparent age (i.e., the aquifer mean transit time, or *MTT*), and the flow-weighted distribution of age (i.e., the transit time distribution, or *TTD*), in the groundwater discharge from the aquifer.

Results from two field campaigns show good agreement in *MTT* based on ^{3}H/^{3}He ages (29–31 years, Table 3), from both closely spaced point measurements in a 58 m reach during low flow and more widely dispersed point measurements in a 2.5 km reach during high flow. These *MTT* values agreed closely with those determined in previous streambed sampling [*Kennedy et al.*, 2009a], even though we used different tracers and detected younger ($<$10 years) groundwater discharge by sampling closer to the stream banks. *MTT* estimates from streambed sampling were only slightly older (10–15%) than values derived from sampling groundwater in nearby wells and from a reach mass balance study of SF_6 in West Bear Creek. The reproducibility of *MTT* from various streambed point sampling arrangements and reasonable agreement with the more traditional well sampling approach suggest that streambed point sampling can be a robust alternative to more traditional well sampling for estimation of groundwater *MTT*.

The *TTDs* from streambed point sampling were well fit by a gamma distribution with values of 10–18 for the shape parameter (Figure 4), large values relative to α values less than 1 that have been observed for transit time distributions on small watersheds [e.g., *Kirchner et al.*, 2000, 2010]. *MTT* estimated by fitting a gamma distribution to the age data was within 1–3 years of the *MTT* values computed as flow-weighted mean apparent ages. The exponential-piston flow model (EPM) based on confined groundwater flow without recharge downgradient of unconfined flow with recharge did not fit the measured *TTD* as well as the

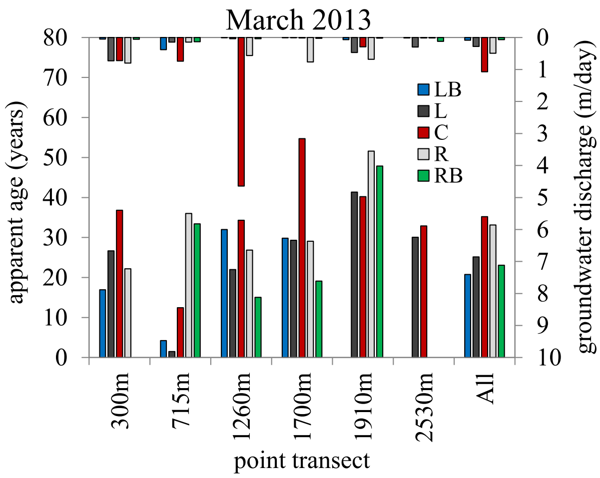

Figure 7. Apparent groundwater age from streambed point sampling (n = 26), and groundwater discharge (used to weight ages when calculating *MTT*), March 2013. Ages are from $^3H/^3He$, and from SF_6 for three points at which $^3H/^3He$ was unavailable. Groundwater age could not be calculated for two samples that were lost during analysis (2530R and 2530RB) and two others with anomalously high or low noble gas concentrations (1260L and 2530LB, respectively). Age of zero was estimated for the point sample collected at 300RB. Blankets were deployed along the 715 m transect.

gamma model, but both models were much closer to the data than the exponential model (EM) often assumed for unconfined aquifers and based in part on uniform recharge. The superior fit of the gamma model has important implications for transport of nonpoint-source pollutants through surficial unconfined aquifers and into surface water, e.g., compared to the EM, the observed gamma *TTD* suggests that nitrate output from the groundwater system to streams would initially respond much more slowly to a reduction in N loading at the land surface, but then nitrate output would drop steadily for about 20 years (in this relatively narrow *TTD*, ~76% of groundwater discharge to West Bear Creek was 20–40 years old), and not show the problematic decades-long tailing behavior characteristic of an exponential distribution.

The better fit of EPM compared to EM suggests that spatial variation in recharge may be important to the observed *TTD* of surficial aquifers; the good fit of the gamma model suggests that the values of its parameters α and β (equation (7)) for a given aquifer may be related to the spatial distribution of recharge to the aquifer. We hypothesize that the relatively small flux of young water through the streambed of West Bear Creek (~12% of groundwater discharge was <20 years old), a major feature of the observed *TTD*, may be linked to low recharge near the stream. The poorly drained soils and shallow low-permeability layer in the floodplain likely cause the groundwater system to operate there as a semiconfined aquifer through which groundwater flow increases in mean age due to little addition of modern water before discharge to the stream. Discharge of younger groundwater likely occurs at locations other than the mainly horizontal streambed of the main channel, such as agricultural ditches, tributaries, or steep near-vertical faces just above or below the waterline on the stream banks. Including such locations in future sampling efforts may give a fuller picture of groundwater *TTD* and *MTT* in the watershed.

Apparent groundwater age was generally older for point samples compared to blanket samples, due at least in part to the presence of some surface water in samples of blanket discharge (e.g., Figure 3). Tracer data from most point and corrected blanket samples suggested it was reasonable to use a piston flow model to estimate groundwater ages for individual samples (Appendix A), but streambed seepage devices in general may require more complex analyses (e.g., correcting for stream water in samples, or the greater probability for mixed groundwater samples). As a whole, our results from two field campaigns suggest that groundwater collected in the streambed may provide reasonable estimates of apparent groundwater age, and that *MTT* can be determined from different age-dating tracers and from sampling with different groundwater collection devices. Coupled streambed point measurements of groundwater age and groundwater seepage rate represent a novel, reproducible, and effective approach to estimating aquifer *TTD* as well as *MTT*.

Appendix

Testing for extensive groundwater mixing has commonly been accomplished with tracer plots. Plots comparing initial tritium ($[^3H]+[^3He_{trit}]=[^3H_{initial}]$) to ^3H in precipitation (Figure A1) are commonly used to evaluate the appropriateness of $^3H/^3He$ apparent ages [eg., *Friedrich et al.*, 2013; *Visser et al.*, 2013, 2007; *Happell et al.*, 2006; *Koh et al.*, 2006; *Price et al.*, 2003; *Shapiro et al.*, 1999; *Aeschbach-Hertig et al.*, 1998; *Stute et al.*, 1997; *Ekwurzel et al.*, 1994; *Dunkle et al.*, 1993]. No local long-term record of ^3H was available, so we compared our $[^3H_{initial}]$ to ^3H data from Cape Hatteras, NC, and Washington, DC, precipitation. Cape Hatteras is

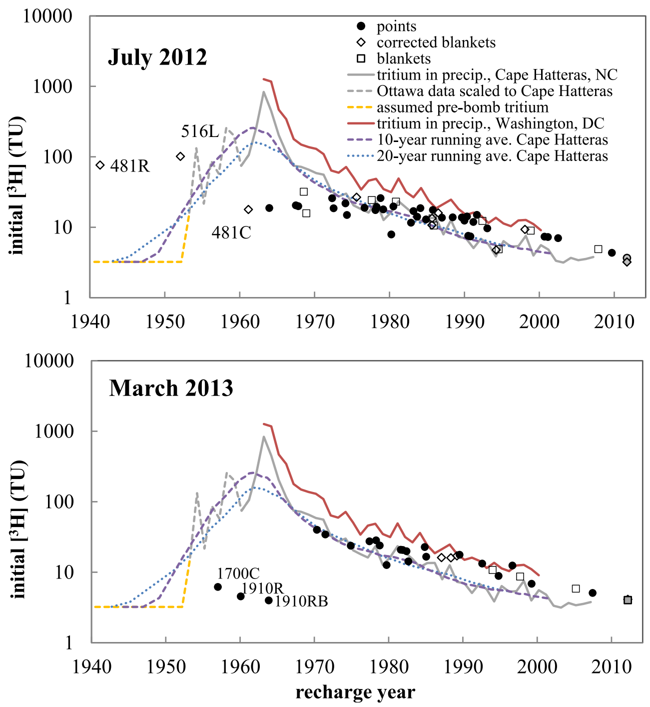

Figure A1. Reconstructed initial (recharge) tritium in July 2012 and March 2013 samples, from modeled [$^3He_{trit}$] and measured [^3H], plotted with [^3H] measured in precipitation at Cape Hatteras, NC, and Washington, DC. [^3H] data from Cape Hatteras, NC, precipitation were not available for recharge years prior to 1960. [^3H] in Cape Hatteras precipitation for recharge years 1954–1960 was estimated using the published correlations with Vienna, Austria, ^3H data for Cape Hatteras [*International Atomic Energy Agency*, 1992]. For recharge years prior to 1954, background [^3H] was assumed to be 5 TU in Vienna [*Kaufman and Libby*, 1954], which correlated to 3.2 TU at Cape Hatteras, NC. The "10 year running ave." curve is the 10 year running average of initial [^3H] from Cape Hatteras, NC, plotted against the running average apparent age from $^3H/^3He$, after *Aeschbach-Hertig et al.* [1998]. The "20 year running ave." curve was plotted in the same manner. Light gray filled symbols indicate samples where modeled [$^3He_{trit}$] < 0 and apparent age was set $= 0$ years.

closer to the study site, but is a coastal observation site and may therefore slightly underestimate precipitation ^3H at West Bear Creek (probably by $<10\%$) [e.g., *Ingraham*, 2006, Figure 3.16]. Washington, DC, data may slightly overestimate precipitation ^3H at West Bear Creek (perhaps by $\sim$20%) [*Ferronsky and Polyakov*, 2012, Figure 13.15], given that it is a similar distance from the coast but about 400 km north of West Bear Creek.

Deviations of [$^3H_{initial}$] in groundwater from the ^3H precipitation curve are usually attributed to (1) dispersion in the groundwater system, which broadens and flattens the bomb peak, (2) mixing of pre-bomb-peak and post-bomb-peak water, which usually causes [$^3H_{initial}$] to plot below the ^3H precipitation curve, or (3) loss of ^3He. ^3He loss could be due to degassing in the ground, artifacts of sampling or analysis, or diffusion. Diffusive losses of ^3He across the water table may occur when recharge rates are low (e.g., $<$30 mm/yr [*Solomon and Cook*, 2000]), and/or during recharge years when the bomb-peak ^3H was entering the groundwater system [*Solomon et al.*, 1993] and $^3He_{trit}$ concentration gradients were large. Deviations of our [$^3H_{initial}$] estimates from the ^3H precipitation curve (Figure A1) were mostly similar in magnitude to deviations observed in previously published groundwater data [eg., *Friedrich et al.*, 2013; *Visser et al.*, 2013, 2007; *Koh et al.*, 2006; *Price et al.*, 2003; *Shapiro et al.*, 1999; *Aeschbach-Hertig et al.*, 1998; *Stute et al.*, 1997; *Ekwurzel et al.*, 1994; *Dunkle et al.*, 1993], and could be explained by dispersion typical of clastic aquifers.

Mixtures representing a range of groundwater age (e.g., 10–20 year range) are not distinguishable from unmixed groundwater samples over much of the ^3H precipitation curve (Figure A1) [*Aeschbach-Hertig et al*, 1998], but the plot is useful for identifying samples which have been significantly affected by the three processes described above. In March 2013, three groundwater point samples from the downstream end of the 2.5 km reach, apparently recharged during 1955–1965, stand out because [$^3H_{initial}$] is very low (Figure A1) The low [$^3H_{initial}$] suggests that the samples may have actually contained a fraction of groundwater recharged before 1953, and is consistent with the elevated $^4He_{terr}$ in the samples (high ^4He is associated with older groundwater, and the mean [^4He] in these samples was 3 times the mean [^4He] in March 2013). The small amounts of $^3He_{trit}$ and ^3H in the samples from the 1700C, 1910R, and 1910RB locations may be from mixing or diffusion of ^3He and ^3H from younger groundwater. Removing these three apparent age estimates from the March 2013 *MTT* calculation reduced *MTT* by 1.3 years (to 29.7 years). The detection of a ^3H-free fraction within these groundwater samples could be conceptually important, given recent studies suggesting the potential importance of old groundwater discharge to streamflow in some hydrologic systems [e.g., *Genereux et al.*, 2009; *Gardner et al.*, 2011], including significant tailing in residence time distributions in field and/or numerical studies [e.g., *Cirpka et al.*, 2007; *Frisbee et al.*, 2013, *Sawyer and Cardenas*, 2009; *Green et al.*, 2010]. Due to the limited range of the age-dating tracers used in this study, we cannot

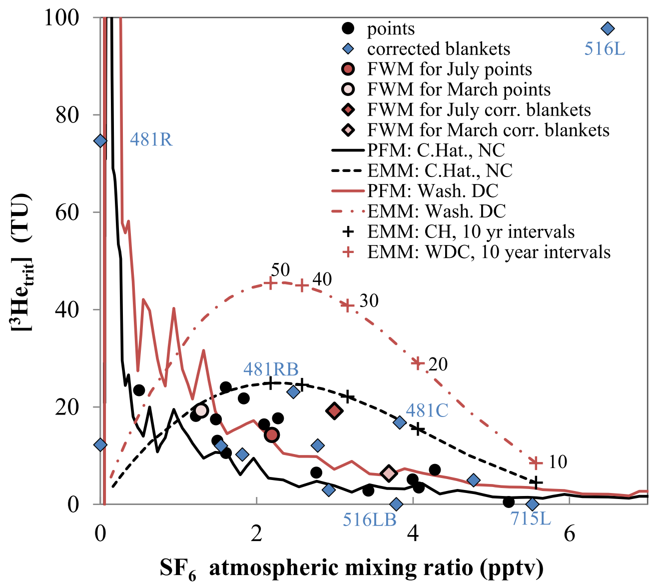

Figure A2. Atmospheric mixing ratios modeled from streambed point and streambed blanket dissolved gas data plotted with the measured atmospheric mixing ratio curve (piston-flow model, PFM) and calculated mixing ratio curve from the exponential mixing model (EM) equation. PFM and EM models were used to predict [$^3He_{trit}$] for sampling in 2013, based on [^3H] from Cape Hatteras, NC (C.Hat., NC), and Washington, DC (Wash. DC). Crosses on the EM lines indicate 10 year *MTT* intervals, beginning at 10 years on the right side of the figure. Blue data labels correspond to corrected blanket data. For 481R, correcting blanket data resulted in an [SF_6] of −0.9 pptv (the concentration is shown here as zero). Corrected data from 516LB and 715L blanket locations showed slightly negative [$^3He_{trit}$] (−0.4 and −1.5 TU, respectively) and both were interpreted as [$^3He_{trit}$] = 0 for the purpose of estimating age from $^3H/^3He$. Flow-weighted mean (FWM) concentrations for points and corrected blankets are also shown.

rule out that small fractions of pretracer (roughly pre-1950) groundwater may have been present in these three (and other) samples collected in the streambed of West Bear Creek. If several samples contained pretracer groundwater, the cumulative effect would be that the "true" *TTD* for groundwater entering West Bear Creek would have greater tailing toward higher transit times than depicted in Figure 4, and the "true" *MTT* would be greater than shown in Table 3.

One corrected blanket sample (481R) stood out in the July 2012 data set (Figure A1) because the apparent age suggested recharge prior to the bomb ^3H peak, but [$^3H_{initial}$] was very high. Corrections to [SF_6] and all CFC concentrations resulted in negative age-dating tracer concentrations for water from the blanket at 481R. Uncertainty in the correction calculation (based on analytical and model uncertainties) was in the range of 9–30% for [^3H], [$^3He_{trit}$], and [SF_6], suggesting that some artifact that is unaccounted for in the uncertainty analysis (e.g., issues with blanket installation or sampling) is likely responsible. Corrected data from the blanket sampled at 516L also gave high [$^3H_{initial}$], but the value plotted close to the ^3H input curve. The corrected data from the blanket at 516L also showed high SF_6 concentration (corresponding to young water) compared to the large amount of [$^3He_{trit}$] (corresponding to older water) (Figure A2). Estimated uncertainty in corrected tracer concentrations for the 516L blanket ranged from 18 to 50%. The range of uncertainty in corrected tracer concentrations for the 481C blanket, which stood out in both Figure A1 (low [$^3H_{initial}$]) and Figure A2 (discussed below), ranged from 6 to 42%.

Two blanket samples plotted near the exponential model (EM) curve for Cape Hatteras (Figure A2). For the 481RB sample, the PFM age was 36.1 years compared to an *MTT* of about 42 years from the EM curve; for the 481C sample, the apparent age could be interpreted as 50 years (PFM) or 22 years (EM). With the exception of July 2012 corrected blanket data (biased somewhat by the 516L blanket data), the flow-weighted mean concentrations from points and corrected blanket data plotted near the PFM (Figure A2). Of course, blanket sampling includes by design some integration/mixing of flow paths at the sampling device, which is inherently different than the natural process of mixing by dispersion during groundwater flow; apparently, near linearity of tracer concentrations versus age for some (but not all) tracers and time periods will produce integrated blanket samples that plot near PFM curves (Figure A2).

Finally, we note that point sampling in the presence of lateral gradients in groundwater age in the streambed likely led to only a small amount of mixing of groundwaters of different age in individual samples. Visualizing the point-scale groundwater sampling as drawing a spherical volume of groundwater toward the 5 cm piezomanometer screens through a sandy streambed of porosity 0.35, the "sampling radius" (radius of the spherical groundwater volume sampled) ranged from 11 cm (for points without CFC and SF_6 sampling) to 17 cm (for points with CFC and SF_6 sampling). Based on the mean streambed groundwater age gradient of 10.6 yr/m of horizontal distance, the first and last groundwater sampled would differ in age by 1.2 or 1.8 years for sampling radii of 11 and 17 cm, respectively, and the last groundwater sampled may span an age range of twice this much (2.4 and 3.6 year) if age varies laterally across the full spherical streambed volume sampled. These are upper limits based on the entire groundwater sampling volume at each point, which included purge water, basic water quality parameters with an in-line flow cell, and samples for other constituents (cations, anions, nitrate, and Si) before collection of samples for age analysis. The age range would likely be much smaller in any single groundwater sample for age-dating tracer analysis, making this form of mixing a minor contributor to uncertainty in individual apparent ages.

Acknowledgments
Data used for tables and figures are available from the corresponding author upon request. This project was funded by National Science Foundation under awards EAR-1045162 to North Carolina State University and EAR-1045134 to the University of Utah. The authors gratefully acknowledge assistance with field work: Matt Burnette and Scott Becker (both NC State) and Briant Kimball (USGS, retired) in July 2012 and March 2013 and Casey Kennedy (USDA-ARS) and Matt Webb (Arcadis U.S.) in March 2013. We also gratefully acknowledge the anonymous reviewers who contributed significantly to the quality of the manuscript

References

Aeschbach-Hertig, W., and D. K. Solomon (2013), Noble gas thermometry in groundwater hydrology, in *The Noble Gases as Geochemical Tracers*, edited by P. Burnard, pp. 81–122, Springer, Heidelberg, Germany.

Aeschbach-Hertig, W., P. Schlosser, M. Stute, H. J. Simpson, A. Ludin, and J. F. Clark (1998), A ^{3}H/^{3}He study of ground water flow in a fractured bedrock aquifer, *Ground Water*, *36*(4), 661–670, doi:10.1111/j.1745-6584.1998.tb02841.x.

Aeschbach-Hertig, W., H. El-Gamal, M. Wieser, and L. Palcsu (2008), Modeling excess air and degassing in groundwater by equilibrium partitioning with a gas phase, *Water Resour. Res.*, *44*, W08449, doi:10.1029/2007WR006454.

Amin, I. E., and M. E. Campana (1996), A general lumped parameter model for the interpretation of tracer data and transit time calculation in hydrologic systems, *J. Hydrol.*, *179*(1–4), 1–21, doi:10.1016/0022-1694(95)02880-3.

Andrews, L. C., and R. L. Phillips (2003), *Mathematical Techniques for Engineers and Scientists*, SPIE—The Int. Soc. for Opt. Eng., Bellingham, Wash.

Bethke, C. M., and T. M. Johnson (2008), Groundwater age and groundwater age dating, *Annu. Rev. Earth Planet. Sci.*, *36*(1), 121–152, doi:10.1146/annurev.earth.36.031207.124210.

Böhlke, J. K., and J. M. Denver (1995), Combined use of groundwater dating, chemical and isotopic analyses to resolve the history and fate of nitrate contamination in two agricultural watersheds, Atlantic coastal plain, Maryland, *Water Resour. Res.*, *31*(9), 2319, doi:10.1029/95WR01584.

Böhlke, J. K., R. Wanty, M. Tuttle, G. Delin, and M. Landon (2002), Denitrification in the recharge area and discharge area of a transient agricultural nitrate plume in a glacial outwash sand aquifer, Minnesota, *Water Resour. Res.*, *38*(7), doi:10.1029/2001WR000663.

Browne, B. A., and N. M. Guldan (2005), Understanding long-term baseflow water quality trends using a synoptic survey of the ground water-surface water interface, Central Wisconsin, *J. Environ. Qual.*, *34*(3), 825–35.

Bullister, J. L., D. P. Wisegarver, and F. A. Menzia (2002), The solubility of sulfur hexafluoride in water and seawater, *Deep Sea Res., Part I*, *49*(1), 175–187, doi:10.1016/S0967-0637(01)00051-6.

Busenberg, E., and L. N. Plummer (2000), Dating young groundwater with sulfur hexafluoride: Natural and anthropogenic sources of sulfur hexafluoride, *Water Resour. Res.*, *36*(10), 3011–3030, doi:10.1029/2000WR900151.

Cirpka, O. A., M. N. Fienen, M. Hofer, E. Hoehn, A. Tessarini, R. Kipfer, and P. K. Kitanidis (2007), Analyzing bank filtration by deconvoluting time series of electrical conductivity, *Ground Water*, *45*(3), 318–328, doi:10.1111/j.1745-6584.2006.00293.x.

Dunkle, S. A., L. N. Plummer, E. Busenberg, P. J. Phillips, J. M. Denver, P. A. Hamilton, R. L. Michel, and T. B. Coplen (1993), Chlorofluorocarbons (CCl_3F and CCl_2F_2) as dating tools and hydrologic tracers in shallow groundwater of the Delmarva Peninsula, Atlantic Coastal Plain, United States, *Water Resour. Res.*, *29*(12), 3837–3860, doi:10.1029/93WR02073.

Ekwurzel, B., P. Schlosser, W. M. Smethie, L. N. Plummer, E. Busenberg, R. L. Michel, R. Weppernig, and M. Stute (1994), Dating of shallow groundwater: Comparison of the transient tracers ^{3}H/^{3}He, chlorofluorocarbons, and ^{85}Kr, *Water Resour. Res.*, *30*(6), 1693–1708, doi:10.1029/94WR00156.

Ferronsky, V. I., and V. A. Polyakov (2012), *Isotopes of the Earth's Hydrosphere [online]*, Springer, Dordrecht, Netherland. [Available at http://catalog.lib.ncsu.edu/record/NCSU2693065.]

Friedrich, R., G. Vero, C. von Rohden, B. Lessmann, R. Kipfer, and W. Aeschbach-Hertig (2013), Factors controlling terrigenic SF_6 in young groundwater of the Odenwald region (Germany), *Appl. Geochem.*, *33*, 318–329, doi:10.1016/j.apgeochem.2013.03.002.

Frisbee, M. D., J. L. Wilson, J. D. Gomez-Velez, F. M. Phillips, and A. R. Campbell (2013), Are we missing the tail (and the tale) of residence time distributions in watersheds?, *Geophys. Res. Lett.*, *40*(17), 4633–4637, doi:10.1002/grl.50895.

Gardner, W. P., G. A. Harrington, D. K. Solomon, and P. G. Cook (2011), Using terrigenic 4He to identify and quantify regional groundwater discharge to streams, *Water Resour. Res.*, *47*, W06523, doi:10.1029/2010WR010276.

Genereux, D. P., S. Leahy, H. Mitasova, C. D. Kennedy, and D. R. Corbett (2008), Spatial and temporal variability of streambed hydraulic conductivity in West Bear Creek, North Carolina, USA, *J. Hydrol.*, *358*(3–4), 332–353, doi:10.1016/j.jhydrol.2008.06.017.

Genereux, D. P., M. Webb, and D. K. Solomon (2009), Chemical and isotopic signature of old groundwater and magmatic solutes in a Costa Rican rain forest: Evidence from carbon, helium, and chlorine, *Water Resour. Res.*, *45*, W08413, doi:10.1029/2008WR007630.

Gilmore, T. E. (2015), *Groundwater transit times and the fate of aquifer nitrate: Observations from sampling in stream channels and well nests in an agricultural watershed,* North Carolina, USA, PhD dissertation, 226 pp., Dep. of Biol. and Agric. Eng., N. C. State Univ., Raleigh. [Available at http://repository.lib.ncsu.edu/ir/bitstream/1840.16/10373/1/etd.pdf.]

Gilmore, T. E., D. P. Genereux, D. K. Solomon, J. E. Solder, B. A. Kimball, H. Mitasova, and F. Birgand (2016), Quantifying the fate of agricultural nitrogen in an unconfined aquifer: stream-based observations at three measurement scales, *Water Resour. Res.*, *52*, doi:10.1002/2015WR017599.

Green, C. T., J. K. Böhlke, B. A. Bekins, and S. P. Phillips (2010), Mixing effects on apparent reaction rates and isotope fractionation during denitrification in a heterogeneous aquifer, *Water Resour. Res.*, *46*, W08525, doi:10.1029/2009WR008903.

Green, C. T., Y. Zhang, B. C. Jurgens, J. J. Starn, and M. K. Landon (2014), Accuracy of travel time distribution (TTD) models as affected by TTD complexity, observation errors, and model and tracer selection, *Water Resour. Res.*, *50*, 6191–6213, doi:10.1002/2014WR015625.

Hamilton, S. K. (2012), Biogeochemical time lags may delay responses of streams to ecological restoration, *Freshwater Biol.*, *57*, 43–57, doi:10.1111/j.1365-2427.2011.02685.x.

Happell, J. D., S. Opsahl, Z. Top, and J. P. Chanton (2006), Apparent CFC and ^{3}H/^{3}He age differences in water from Floridan Aquifer springs, *J. Hydrol.*, *319*(1–4), 410–426, doi:10.1016/j.jhydrol.2005.07.033.

Hrachowitz, M., C. Soulsby, D. Tetzlaff, I. A. Malcolm, and G. Schoups (2010), Gamma distribution models for transit time estimation in catchments: Physical interpretation of parameters and implications for time-variant transit time assessment, *Water Resour. Res.*, *46*, W10536, doi:10.1029/2010WR009148.

Ingraham, N. L. (2006), Isotopic variations in precipitation, in *Isotope Tracers in Catchment Hydrology*, edited by C. Kendall and J. J. McDonnell, pp. 87–118, Elsevier, Boston, Mass.

International Atomic Energy Agency (1992), Statistical treatment of isotope data in precipitation, *Tech. Rep. 206*, 255 pp., Vienna.

Kaufman, S., and W. F. Libby (1954), The natural distribution of tritium, *Phys. Rev.*, *93*(6), 1337–1344, doi:10.1103/PhysRev.93.1337.

Kennedy, C. D., D. P. Genereux, D. R. Corbett, and H. Mitasova (2007), Design of a light-oil piezomanometer for measurement of hydraulic head differences and collection of groundwater samples, *Water Resour. Res.*, *43*, W09501, doi:10.1029/2007WR005904.

Kennedy, C. D., D. P. Genereux, H. Mitasova, D. R. Corbett, and S. Leahy (2008), Effect of sampling density and design on estimation of streambed attributes, *J. Hydrol.*, *355*, 164–180, doi:10.1016/j.jhydrol.2008.03.018.

Kennedy, C. D., D. P. Genereux, D. R. Corbett, and H. Mitasova (2009a), Relationships among groundwater age, denitrification, and the coupled groundwater and nitrogen fluxes through a streambed, *Water Resour. Res.*, *45*, W09402, doi:10.1029/2008WR007400.

Kennedy, C. D., D. P. Genereux, D. R. Corbett, and H. Mitasova (2009b), Spatial and temporal dynamics of coupled groundwater and nitrogen fluxes through a streambed in an agricultural watershed, *Water Resour. Res.*, *45*, W090401, doi:10.1029/2008WR007397.

Kennedy, C. D., L. C. Murdoch, D. P. Genereux, D. R. Corbett, K. Stone, P. Pham, and H. Mitasova (2010), Comparison of Darcian flux calculations and seepage meter measurements in a sandy streambed in North Carolina, United States, *Water Resour. Res.*, *46*, W09501, doi:10.1029/2009WR008342.

Kirchner, J. W., X. Feng, and C. Neal (2000), Fractal stream chemistry and its implications for contaminant transport in catchments, *Nature*, *403*(6769), 524–527, doi:10.1038/35000537.

Kirchner, J. W., D. Tetzlaff, and C. Soulsby (2010), Comparing chloride and water isotopes as hydrological tracers in two Scottish catchments, *Hydrol. Processes*, *24*(12), 1631–1645, doi:10.1002/hyp.7676.

Koh, D. C., L. Niel Plummer, D. K. Solomon, E. Busenberg, Y. J. Kim, and H. W. Chang (2006), Application of environmental tracers to mixing, evolution, and nitrate contamination of ground water in Jeju Island, Korea, *J. Hydrol.*, *327*(1–2), 258–275, doi:10.1016/j.jhydrol.2005.11.021.

Kollet, S. J., and R. M. Maxwell (2008), Demonstrating fractal scaling of baseflow residence time distributions using a fully-coupled groundwater and land surface model, *Geophys. Res. Lett.*, *35*, L07402, doi:10.1029/2008GL033215.

Lindsey, B. D., S. W. Phillips, C. A. Donnelly, G. K. Speiran, L. N. Plummer, J. K. Böhlke, M. J. Focazio, W. C. Burton, and E. Busenberg (2003), Residence times and nitrate transport in ground water discharging to streams in the Chesapeake Bay watershed, *Water Resour. Invest. Rep. 03-4035*, U.S. Geol. Surv., Reston, Va.

Massoudieh, A., S. Sharifi, and D. K. Solomon (2012), Bayesian evaluation of groundwater age distribution using radioactive tracers and anthropogenic chemicals, *Water Resour. Res.*, *48*, W09529, doi:10.1029/2012WR011815.

Massoudieh, A., A. Visser, S. Sharifi, and H. P. Broers (2014), A Bayesian modeling approach for estimation of a shape-free groundwater age distribution using multiple tracers, *Appl. Geochem.*, *50*, 252–264, doi:10.1016/j.apgeochem.2013.10.004.

McCallum, J. L., P. G. Cook, C. T. Simmons, and A. D. Werner (2014), Bias of apparent tracer ages in heterogeneous environments, *Ground Water*, *52*(2), 239–250, doi:10.1111/gwat.12052.

Meals, D. W., S. A. Dressing, and T. E. Davenport (2010), Lag time in water quality response to best management practices: A review, *J. Environ. Qual.*, *39*(1), 85–96, doi:10.2134/jeq2009.0108.

Modica, E., H. T. Buxton, and L. N. Plummer (1998), Evaluating the source and residence times of groundwater seepage to streams, New Jersey Coastal Plain, *Water Resour. Res.*, *34*(11), 2797–2810, doi:10.1029/98WR02472.

Molénat, J., C. Gascuel-Odoux, L. Aquilina, and L. Ruiz (2013), Use of gaseous tracers (CFCs and SF_6) and transit-time distribution spectrum to validate a shallow groundwater transport model, *J. Hydrol.*, *480*, 1–9, doi:10.1016/j.jhydrol.2012.11.043.

Plummer, L. N., and E. Busenberg (2000), Chloroflurocarbons, in *Environmental Tracers in Subsurface Hydrology*, edited by P. G. Cook and A. Herczeg, pp. 441–478, Kluwer Acad., Boston, Mass

Plummer, L. N., E. Busenberg, and P. G. Cook (2006), Principles of chlorofluorocarbon dating, in *Use of Chlorofluorocarbons in Hydrology: A Guidebook*, edited by E. Busenberg, pp. 17–30, Int. At. Energy Agency, Vienna.

Poreda, R. J., T. E. Cerling, and D. K. Salomon (1988), Tritium and helium isotopes as hydrologic tracers in a shallow unconfined aquifer, *J. Hydrol.*, *103*(1–2), 1–9, doi:10.1016/0022-1694(88)90002-9.

Portniaguine, O., and D. K. Solomon (1998), Parameter estimation using groundwater age and head data, Cape Cod, Massachusetts, *Water Resour. Res.*, *34*(4), 637–645, doi:10.1029/97WR03361.

Price, R. M., Z. Top, J. D. Happell, and P. K. Swart (2003), Use of tritium and helium to define groundwater flow conditions in Everglades National Park, *Water Resour. Res.*, *39*(9), 1267, doi:10.1029/2002WR001929.

Puckett, L. J. (2004), Hydrogeologic controls on the transport and fate of nitrate in ground water beneath riparian buffer zones: Results from thirteen studies across the United States, *Water Sci. Technol.*, *49*(3), 47–53.

Reilly, T. E., L. N. Plummer, P. J. Phillips, and E. Busenberg (1994), The use of simulation and multiple environmental tracers to quantify groundwater flow in a shallow aquifer, *Water Resour. Res.*, *30*(2), 421–433, doi:10.1029/93WR02655.

Sanford, W. (2011), Calibration of models using groundwater age, *Hydrogeol. J.*, *19*(1), 13–16, doi:10.1007/s10040-010-0637-6.

Sanford, W. E., and J. P. Pope (2013). Quantifying groundwater's role in delaying improvements to Chesapeake Bay water quality, *Environ. Sci. Technol.*, *47*(23), 13,330–13,338, doi:10.1021/es401334k.

Sawyer, A. H., and M. B. Cardenas (2009), Hyporheic flow and residence time distributions in heterogeneous cross-bedded sediment, *Water Resour. Res.*, *45*, W08406, doi:10.1029/2008WR007632.

Schlosser, P., M. Stute, H. Dörr, C. Sonntag, and K. O. Münnich (1988), Tritium/^{3}He dating of shallow groundwater, *Earth Planet. Sci. Lett.*, *89*(3–4), 353–362, doi:10.1016/0012-821X(88)90122-7.

Shapiro, S. D., D. LeBlanc, P. Schlosser, and A. Ludin (1999), Characterizing a sewage plume using the ^{3}H-^{3}He dating technique, *Ground Water*, *37*(6), 861–878, doi:10.1111/j.1745-6584.1999.tb01185.x.

Solder, J. E. E. (2014), Quantifying groundwater-surface water exchange: Development and testing of shelby tubes and seepage blankets as discharge measurement and sample collections devices, MS thesis, Univ. of Utah, Salt Lake City. [Available at http://content.lib.utah.edu/cdm/singleitem/collection/etd3/id/3170/rec/1.]

Solomon, D. K., and P. G. Cook (2000), ^{3}H and ^{3}He, in *Environmental Tracers in Subsurface Hydrology*, edited by P. G. Cook and A. Herczeg, pp. 397–424, Kluwer Acad., Boston, Mass.

Solomon, D. K., and E. A. Sudicky (1991), Tritium and Helium 3 isotope ratios for direct estimation of spatial variations in groundwater recharge, *Water Resour. Res.*, *27*(9), 2309–2319, doi:10.1029/91WR01446.

Solomon, D. K., S. L. Schiff, R. J. Poreda, and W. B. Clarke (1993), A validation of the ^{3}H/^{3}He method for determining groundwater recharge, *Water Resour. Res.*, *29*(9), 2951–2962, doi:10.1029/93WR00968.

Solomon, D. K., P. G. Cook, and L. N. Plummer (2006), Models of groundwater ages and residence times, in *Use of Chlorofluorocarbons in Hydrology: A Guidebook*, edited by E. Busenberg, pp. 73–78, Int. At. Energy Agency, Vienna.

Solomon, D. K., T. E. Gilmore, J. E. Solder, B. Kimball, and D. P. Genereux (2015), Evaluating an unconfined aquifer by analysis of age-dating tracers in stream water, *Water Resour. Res.*, *51*, 8883–8899, doi:10.1002/2015WR017602.

Stolp, B. J., D. K. Solomon, A. Suckow, T. Vitvar, D. Rank, P. K. Aggarwal, and L. F. Han (2010), Age dating base flow at springs and gaining streams using helium-3 and tritium: Fischa-Dagnitz system, southern Vienna Basin, Austria, *Water Resour. Res.*, *46*, W07503, doi:10.1029/2009WR008006.

Stute, M., J. Deák, K. Révész, J. K. Böhlke, E. Deseö, R. Weppernig, and P. Schlosser (1997), Tritium/^{3}He dating of river infiltration: An example from the Danube in the Szigetköz area, Hungary, *Ground Water*, *35*(5), 905–911, doi:10.1111/j.1745-6584.1997.tb00160.x.

Tesoriero, A. J. (2005), Nitrogen transport and transformations in a coastal plain watershed: Influence of geomorphology on flow paths and residence times, *Water Resour. Res.*, *41*, W02008, doi:10.1029/2003WR002953.

Tesoriero, A. J., J. H. Duff, D. A. Saad, N. E. Spahr, and D. M. Wolock (2013), Vulnerability of streams to legacy nitrate sources, *Environ. Sci. Technol.*, *47*(8), 3623–3629, doi:10.1021/es305026x.

Visser, A., H. P. Broers, and M. F. P. Bierkens (2007), Dating degassed groundwater with ^{3}H/^{3}He, *Water Resour. Res.*, *43*, W10434, doi:10.1029/2006WR005847.

Visser, A., H. P. Broers, R. Purtschert, J. Sültenfuß, and M. de Jonge (2013), Groundwater age distributions at a public drinking water supply well field derived from multiple age tracers (^{85}Kr, ^{3}H/^{3}He, and ^{39}Ar), *Water Resour. Res.*, *49*, 7778–7796, doi:10.1002/2013WR014012.

Vogel, J. C. (1967), Investigation of groundwater flow with radiocarbon, in *Isotopes in Hydrology*, pp. 355–369, Int. At. Energy Agency, Vienna.

Weeks, E. P., D. W. Ericson, and C. L. R. Holt (1965), Hydrology of the Little Plover River basin, Portage County, Wisconsin, and the effects of water resources development, *U.S. Geol. Surv. Water Supply Pap.*, *1811*, 78 pp.

Weiss, R. F. (1970), The solubility of nitrogen, oxygen and argon in water and seawater, *Deep Sea Res. Oceanogr. Abstr.*, *17*(4), 721–735, doi:10.1016/0011-7471(70)90037-9.

Weiss, R. F. (1971), Solubility of helium and neon in water and seawater, *J. Chem. Eng. Data*, *16*(2), 235–241, doi:10.1021/je60049a019.

Winner, M. D., and R. W. Coble (1996), Hydrogeologic framework of the North Carolina coastal plain, *U.S. Geol. Surv. Prof. Pap.*, *1404-I*, 119 pp.